A statistical *RCL* interconnect delay model taking account of process variations*

Zhu Zhang-Ming(朱樟明)†, Wan Da-Jing(万达经),
Yang Yin-Tang(杨银堂), and En Yun-Fei(恩云飞)

Microelectronics School, Xidian University, Xi'an 710071*, China*

(Received 30 March 2010; revised manuscript received 23 August 2010)

As the feature size of the CMOS integrated circuit continues to shrink, process variations have become a key factor affecting the interconnect performance. Based on the equivalent Elmore model and the use of the polynomial chaos theory and the Galerkin method, we propose a linear statistical RCL interconnect delay model, taking into account process variations by successive application of the linear approximation method. Based on a variety of nano-CMOS process parameters, HSPICE simulation results show that the maximum error of the proposed model is less than 3.5%. The proposed model is simple, of high precision, and can be used in the analysis and design of nanometer integrated circuit interconnect systems.

Keywords: process variation, interconnect line, statistical delay, successive linear approximation
PACS: 84.30.–r, 84.30.Bw **DOI:** 10.1088/1674-1056/20/1/018401

1. Introduction

With complementary metal-oxide semiconductor (CMOS) integrated circuits shrinking to the nanometer scale, the impact of process variation on integrated circuit design and manufacture has become critical. Process variations with a random nature will directly result in changes in the physical structure of integrated circuits, thereby affecting their performance. Relevant research has become a hot spot of integrated circuit design and verification.[1−4]

In nano-scale integrated circuits, interconnect delay has become one of the key parameters in high-performance chip design. In order to accurately estimate the interconnect delay, many researchers have proposed a variety of models.[5−9] Among them, the Elmore model[8] has been the mainstream model to estimate interconnect delay in the industry because of its simple form, but it does not consider the inductive effect. Based on the important influence of the inductive effect, Ref. [9] proposed an equivalent Elmore model taking into account the inductance effect by application of the same approximation method used in the Elmore model. However, with the rapid development of semiconductor technology, process variations will give rise to great effects on the interconnect delay which cannot be ignored.[10] The literature above contains errors as a result of not considering process variations. Therefore, we should amend the existing delay models to make them applicable to today's nano-scale integrated circuit design.

In order to correctly estimate the impact of process variations on interconnect delay, this paper presents a linear statistical *RCL* interconnect delay model taking into account process variations. We first introduce polynomial chaos theory and the Galerkin method. Then, based on the equivalent Elmore model, we propose an *RCL* delay analytical model taking into account process variations using the successive linear approximation method. Finally we apply HSPICE to verified the proposed model.

2. Polynomial chaos theory and the Galerkin method

2.1. Polynomial chaos theory

Here we suppose that $z = \{z_1, z_2, \ldots, z_N\}$ are unrelated variables with mean 0 and $F(z)$ is a function of z. At the same time, we suppose that $F(z)$ is a second order random process, i.e., it has a finite variance w.r.t z. This is certainly true for all practical interconnect systems. Based on polynomial chaos theory,[11,12]

*Project supported by the National Natural Science Foundation of China (Grant Nos. 60725415 and 60971066), the National Science & Technology Important Project of China (Grant No. 2009ZX01034-002-001-005), and The National Key Laboratory Foundation (Grant No. ZHD200904).
†Corresponding author. E-mail: zmyh@263.net
© 2011 Chinese Physical Society and IOP Publishing Ltd

we can expand function $F(z)$ as a series in orthogonal polynomials $\Gamma_n(z)$ as follows:

$$F(z) = \sum_{n=0}^{\infty} F_n \Gamma_n(z). \tag{1}$$

Reference [11] has proved the methods and convergence of this technology. The orthogonal property implies

$$\begin{aligned} E(\Gamma_i(z)\Gamma_j(z)) &= \int_D \Gamma_i(z)\Gamma_j(z) p\mathrm{d}f(z)\,\mathrm{d}z \\ &= \begin{cases} 0 & \text{if } i \neq j; \\ 1 & \text{if } i = j; \end{cases} \end{aligned} \tag{2}$$

where D is the range of the variation of z and $p\mathrm{d}f(z)$ is the probability density function of the variable z. It is noteworthy to point out that $\{\Gamma_n(z)\}$ constitutes an orthogonal basis for an infinite dimensional Hilbert space, so for a fixed $z = \{z_1, z_2, \ldots, z_N\}$, function $F(z)$ is a point in the infinite dimensional Hilbert space with orthogonal basis $\{\Gamma_n(z)\}$. There exist different orthogonal polynomials for different distributions of the random variables. If $z = \{z_1, z_2, \ldots, z_N\}$ is in unrelated standard normal distribution, the orthogonal polynomials are Hermite polynomials[12]

$$\begin{aligned} &\mathrm{H}_p\left(\{z_{a_1}, z_{a_2}, \ldots, z_{a_p}\}\right) \\ &= (-1)^p \mathrm{e}^{\frac{1}{2}z^{\mathrm{T}}z} \frac{\partial^p}{\partial z_{a_1}\partial z_{a_2}\ldots\partial z_{a_p}} \mathrm{e}^{\frac{1}{2}z^{\mathrm{T}}z}, \end{aligned} \tag{3}$$

where $\{z_{a_i}\}$ is any set of p variables chosen from the set $\{z_1, z_2, \ldots, z_N\}$ with repetitions. Since p variables can be chosen from a set of N variables in $(p+n-1)!/p!\,(n-1)!$ ways, the number of Hermite polynomials of exact degree p is given by $(p+n-1)!/p!\,(n-1)!$. By calculating, we can obtain that the zero-order and first-order Hermite polynomials for $z = \{z_1, z_2, \ldots, z_N\}$ are $\mathrm{H}_0(\{\}) = 1$ and $\mathrm{H}_1(z_i) = z_i$ respectively. Thus, when $z = \{z_1, z_2, \ldots, z_N\}$ is the unrelated standard normal distribution, $F(z)$ is a point in the infinite-dimensional Hilbert space, and its zero-order and first order orthogonal bases are 1 and $z_i\,(1 \leq i \leq N)$ respectively.

2.2. The Galerkin method

From the above, we can see that for fixed $z = \{z_1, z_2, \ldots, z_N\}$, function $F(z)$ is a point in the infinite-dimensional Hilbert space. For practical computation purposes, the infinite series expansion in Eq. (1) needs to be projected onto a finite-dimensional Hilbert space, i.e. a truncated one. Then it will cause a truncation error. In order to minimise the error, we can apply the Galerkin method.[11]

In practice, we often use the standard normal distribution to model the variable and hope the function $F(z)$ is a linear analytical model. So in this paper, we assume $z = \{z_1, z_2, \ldots, z_N\}$ to be the unrelated standard normal distribution, and map $F(z)$ to a linear approximation model

$$F(z) \approx F_0 + \sum_{j=1}^{N} F_j z_j. \tag{4}$$

The truncation error Δz is

$$\Delta z = F(z) - \left(F_0 + \sum_{j=1}^{N} F_j z_j\right). \tag{5}$$

We use the Galerkin method[11,12] to obtain the coefficients, which essentially states that the truncation error is minimised when the error Δz is orthogonal to the truncation expansion itself.

In other words, when the truncation error Δz is orthogonal to the linear expression $F(z)$, the truncation error Δz is minimised. The orthogonal property is defined in this case as $E(\Delta z \cdot \Gamma_i) = 0$, where $\Gamma_i = \{1, z_1, z_2, \ldots, z_N\}$ in our case. We thus have a set of $N+1$ equations with $N+1$ unknown variables. For example, the first equation is given by $E(\Delta z \cdot 1) = 0$, where

$$\begin{aligned} E(\Delta z \cdot 1) &= \int_{-\infty}^{+\infty} \ldots \int_{-\infty}^{+\infty} \Delta z \cdot p\mathrm{d}f(z)\mathrm{d}z_1 \ldots \mathrm{d}z_N \\ &= \int_{-\infty}^{+\infty} \ldots \int_{-\infty}^{+\infty} \Delta z \cdot \exp\left(-0.5\sum_{0}^{N} z_j^2\right)\mathrm{d}z_1 \ldots \mathrm{d}z_N \\ &= \int_{-\infty}^{+\infty} \ldots \int_{-\infty}^{+\infty} F(z) \cdot p\mathrm{d}f(z)\mathrm{d}z_1 \ldots \mathrm{d}z_N - F_0. \end{aligned} \tag{6}$$

We can obtain the concrete form of F_i $(1 \le i \le N)$ by solving the equations. Substituting F_i into Eq. (4), we obtain the linear approximation expression of $F(z)$. The expression is simple in form and can accurately approximate $F(z)$.

From the above we can see that, when $z = \{z_1, z_2, \ldots, z_N\}$ is the unrelated standard normal distribution, $F(z)$ is a point in the infinite-dimensional Hilbert space. By applying the Galerkin method, we can map function $F(z)$ to the finite-dimensional Hilbert space and obtain a linear approximation function, which is simple and can accurately approximate function $F(z)$.

3. Interconnection parameters taking into account process variations

3.1. The linear approximation model of interconnection parameters taking into account process variations

Any interconnect size fluctuations will affect the parasitic parameters, leading to interconnect delay fluctuations. The impact of process variations on the shape of the interconnection lines is shown in Fig. 1.

In order to model the impact of variability on wire delay, we need to capture the effect of geometric variations on the electrical parameters. The change in electrical parameters due to variations in geometric dimensions can be captured by the simple linear approximation equation[13]

$$\begin{cases} R = R_{\text{nom}} + a_1\Delta W + a_2\Delta T, \\ C = C_{\text{nom}} + b_1\Delta W + b_2\Delta T + b_3\Delta H, \\ L = L_{\text{nom}} + c_1\Delta W + c_2\Delta T. \end{cases} \tag{7}$$

Here, R, C, and L represent respectively the total interconnect resistance per unit length, the total capacitance, and the total inductance taking into account process variations. R_{nom}, C_{nom}, and L_{nom} represent nominal resistance, capacitance, and inductance values, computed when the wire dimensions are at their nominal or typical values ΔW, ΔT, and ΔH represent the change in metal width, metal thickness, and insulated medium thickness respectively. Also, a_i, b_i, and c_i are the model coefficients in the linear model. For simplicity, this paper assumes that ΔW, ΔT, and ΔH obey the unrelated standard normal distribution. For the general normal distribution $X \sim N(\mu, \sigma^2)$, we can carry out the transformation $(X-\mu)/\sigma \sim N(0,1)$, and then we can have the standard normal distribution.

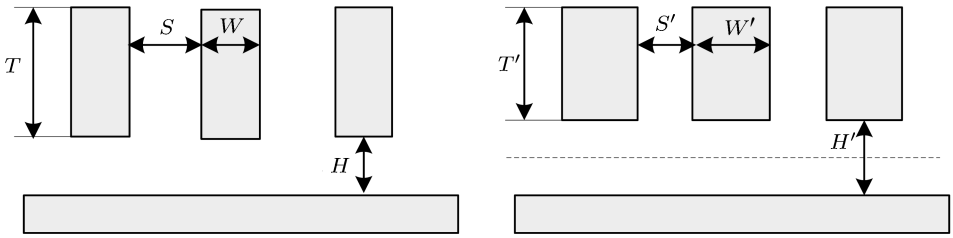


Fig. 1. Interconnection changes caused by process variations.

We can calculate the model parameters a_i, b_i, and c_i through application of the interconnect empirical parasitic model. As shown by the middle line surrounded by two lines in Fig. 1, the line resistance, capacitance, and inductance per unit length can be expressed using the following equations[14,15]

$$R = \rho_{\text{eff}} \frac{1}{WT}, \tag{8}$$

$$\frac{C_{\text{g}}}{\varepsilon_{\text{ox}}} = \left(\frac{2W}{H}\right) + 4.08\left(\frac{T}{T+4.53411H}\right)^{0.071}\left(\frac{S}{S+0.5355H}\right)^{1.773}, \tag{9}$$

$$\frac{C_{\text{c}}}{\varepsilon_{\text{ox}}} = 1.4116\frac{T}{S}\exp\left(-\frac{4S}{S+8.014H}\right) + 2.3704\left(\frac{W}{W+0.3078S}\right)^{0.25724}\left(\frac{H}{H+8.961S}\right)^{0.25724}\exp\left(-\frac{2S}{S+6H}\right), \tag{10}$$

$$L_{\text{self}} = \frac{\mu_0}{2\pi}\left[\ln\left(\frac{2l}{W+T}\right) + \frac{1}{2} + 0.2235\left(\frac{W+T}{l}\right)\right], \quad l >> (W+T); \tag{11}$$

$$L_{\rm mut} = \frac{\mu_0}{2\pi}\left[\ln\left(\frac{2l}{S}\right) - 1 + \frac{S}{l}\right], \quad l > S; \tag{12}$$

where $C_{\rm g}$ and $C_{\rm c}$ are respectively capacitance per unit length between line to ground and line; $L_{\rm self}$ and $L_{\rm mut}$ are respectively self and mutual inductances per unit length; $\rho_{\rm eff}$ is the effective resistivity; $\varepsilon_{\rm ox}$ is the effective dielectric constant; μ_0 is the vacuum magnetic permeability; W, S, T, H, and l are respectively line width, line spacing, line thickness, dielectric thickness, and length of the line. This interconnect empirical parasitic model can accurately estimate the electrical parameters for most materials.[14,15] As in real environments, mutual capacitance and mutual inductance of the interconnect have an important effect on delay, therefore we consider the impact of mutual capacitance and mutual inductance on the accuracy of the estimate of interconnect performance. Therefore the total capacitance and the total inductance per unit length are[14]

$$\begin{cases} C = C_{\rm g} + 2C_{\rm c}, \\ L = L_{\rm self} + 2L_{\rm mut}. \end{cases} \tag{13}$$

Combining Eqs. (8)–(13), the linear modeling coefficients a_i, b_i, and c_i can be readily computed by evaluating the partial derivatives at the nominal point. In order to facilitate the establishment of this model, we suppose that $z = \{z_1, z_2, z_3\} = \{\Delta W, \Delta T, \Delta H\}$, then the resistance, capacitance, and inductance expressions in terms of changes in physical dimensions can now be written as

$$\begin{cases} R = a_0 + \sum\limits_{i=1}^{3} a_i z_i, \\ C = b_0 + \sum\limits_{i=1}^{3} b_i z_i, \\ L = c_0 + \sum\limits_{i=1}^{3} c_i z_i, \end{cases} \tag{14}$$

where

$$\begin{cases} a_0 = R_{\rm nom}, \quad a_1 = \left(\dfrac{\partial R}{\partial W}\right)_{\rm nom}, \\ a_2 = \left(\dfrac{\partial R}{\partial T}\right)_{\rm nom}, \quad a_3 = 0; \\ b_0 = C_{\rm nom}, \quad b_1 = \left(\dfrac{\partial C}{\partial W}\right)_{\rm nom}, \\ b_2 = \left(\dfrac{\partial C}{\partial T}\right)_{\rm nom} \Delta T, \quad b_3 = \left(\dfrac{\partial C}{\partial H}\right)_{\rm nom}; \\ c_0 = L_{\rm nom}, \quad c_1 = \left(\dfrac{\partial L}{\partial W}\right)_{\rm nom}, \\ c_2 = \left(\dfrac{\partial L}{\partial T}\right)_{\rm nom}, \quad c_3 = 0 \end{cases} \tag{15}$$

However, we point out that this formulation is not critical to our approach and any linear models similar to Eq. (14) can be used in our framework. We now discuss how these electrical parameters can be mapped to the moments.

3.2. The linear approximation model of moments taking into account process variations

For the RCL interconnect tree shown in Fig. 2, the moments of each node can be obtained using iterative methods.

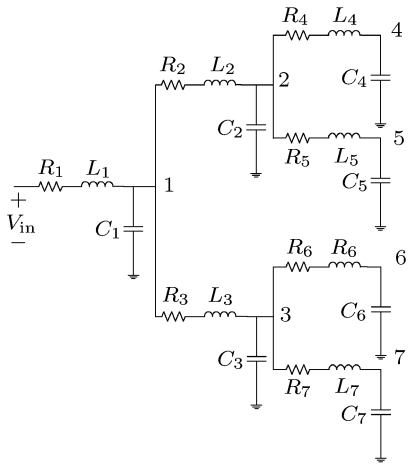


Fig. 2. RCL interconnect tree.

Here we are only interested in the first and second moments. We can express them at node i as follows:[9]

$$\begin{cases} m_1^i = -\sum\limits_k C_k R_{ik}, \\ m_2^i = \sum\limits_k \sum\limits_j C_k R_{ik} C_j R_{kj} - \sum\limits_k C_k L_{ik}. \end{cases} \tag{16}$$

Among them, k is node ordinal number traversing each capacitor in the circuit, R_{ki} and L_{ki} is the public path resistance and inductance from the input to the node i and k. By analysing Eq. (16), we observe that, if we know the linear approximation function $F(z)$, we can obtain the linear approximation function of moments, where

$$F(z) = \left(F_{10} + \sum_{j=1}^{3} F_{1j} z_j\right)\left(F_{20} + \sum_{j=1}^{3} F_{2j} z_j\right). \tag{17}$$

In the formula above, $z = \{z_1, z_2, z_3\}$ is the unrelated standard normal distribution. By applying the

Galerkin method, we can obtain the linear approximation function of $F(z)$

$$F(z) = F_{30} + \sum_{j=1}^{3} F_{3j} z_j, \tag{18}$$

where

$$\begin{aligned} F_{30} &= F_{10}F_{20} + \sum_{j=1}^{3} F_{1j}F_{2j}, \\ F_{3j} &= F_{10}F_{2j} + F_{20}F_{1j}, \quad (1 \le j \le 3). \end{aligned} \tag{19}$$

In practice, users first give the specific expression (16) based on the practical interconnect tree topology. Then, combined with the linear approximation equation (14) of interconnect parameters R, C and L, we can obtain the linear approximation model of moments taking into account process variations by applying the method of Eqs. (17)–(19) on Eq. (16).

$$\begin{cases} m_1^i = m_{10}^i + \sum\limits_{j=1}^{3} m_{1j}^i z_j, \\ m_2^i = m_{20}^i + \sum\limits_{j=1}^{3} m_{2j}^i z_j. \end{cases} \tag{20}$$

4. The statistical *RCL* interconnect delay model taking into account process variations

Among existing delay models, this paper chooses the equivalent Elmore delay model to analyse the impact of process variations on the delay. This model is independent of the specific model of delay although other analytical models can also be applied here. From Ref. [9], we can have the delay model of nodes i in the interconnection trees shown in Figure 2. In order to apply successively the linear approximation method, we express the analytical delay model as follows:

$$\begin{aligned} d &= d_1/\omega_n = (1.047d_2 + 1.39\zeta)/\omega_n \\ &= \left(1.047e^{(\zeta/0.85)} + 1.39\zeta\right)/\omega_n, \end{aligned} \tag{21}$$

where $d_i = d_{i0} + \sum\limits_{j=1}^{3} d_{ij} z_j$, $(1 \le i \le 2)$ is the linear approximation expression of counterpart in Eq. (21), and

$$\begin{aligned} \zeta &= \frac{-m_2}{2}\frac{1}{M_1} = \frac{-m_2}{2}\frac{1}{\sqrt{M_2 - m_2}} \\ &= \frac{-m_2}{2}\frac{1}{\sqrt{m_1^2 - m_2}}, \end{aligned} \tag{22}$$

$$\omega_n = \frac{1}{M_1} = \frac{1}{\sqrt{M_2 - m_2}} = \frac{1}{\sqrt{m_1^2 - m_2}}. \tag{23}$$

In the equation above, m_1 and m_2 are respectively the first moment m_1^i and the second moment m_2^i of node i, of which the specific form is given by Eq. (20). $M_i = M_i(z) = M_{i0} + \sum\limits_{j=1}^{3} M_{ij} z_j$, $(1 \le i \le 2)$ is the linear approximation expression of the counterpart in Eqs. (22) and (23). Based on the Galerkin method, we obtain

$$M_{20} = \sum_{j=0}^{3} m_{1j}^2, \quad M_{2j} = 2m_{10}m_{1j}, \quad (1 \le j \le 3), \tag{24}$$

$$\begin{aligned} M_{10} &= \frac{\sqrt{K_0 - \sqrt{K_0^2 - \sum\limits_{j=1}^{3} K_j^2}}}{\sqrt{2}}, \\ M_{1i} &= \frac{K_i}{\sqrt{2}\sqrt{K_0 - \sqrt{K_0^2 - \sum\limits_{j=1}^{3} K_j^2}}}, \quad (1 \le i \le 3), \end{aligned} \tag{25}$$

where $K_j = M_{2j} - m_{2j}$ $(1 \le j \le 3)$. Here we suppose that the linear approximation expressions of ζ and ω_n are

$$\begin{cases} \zeta = \zeta_0 + \sum\limits_{j=1}^{3} \zeta_j z_j, \\ \omega_n = \omega_{n0} + \sum\limits_{j=1}^{3} \omega_{nj} z_j. \end{cases} \tag{26}$$

Substituting Eqs. (24) and (25) into Eqs. (22) and (23) and applying the Galerkin method, we obtain

$$\begin{aligned} \zeta_0 &= \frac{1}{2}\frac{M_{10}m_{20} - \sum\limits_{j=1}^{3} M_{1j}m_{2j}}{\sum\limits_{j=1}^{3} M_{1j}^2 - M_{10}^2}, \\ \zeta_j &= -\frac{1}{2}\frac{m_{2j}}{M_{10}} - \frac{M_{1j}}{M_{10}}\zeta_0, \quad (1 \le j \le 3); \\ \omega_{n0} &= -\frac{M_{11}}{\sum\limits_{j=1}^{3} M_{1j}^2 - M_{10}^2}, \\ \omega_{nj} &= -\frac{M_{1j}}{M_{10}}\omega_{n0}, \quad (1 \le j \le 3). \end{aligned} \tag{27, 28}$$

Here we substitute Eqs. (26)–(28) into Eq. (21) and apply the Galerkin method, to obtain

$$\begin{aligned} d_{20} &= \exp\left(\zeta_0/0.85 + \sum_{j=1}^{3} (\zeta_j/0.85)^2/4\right), \\ d_{2j} &= \frac{1}{2} d_{20}(\zeta_j/0.85), \quad (1 \le j \le 3); \\ d_{1j} &= 1.047d_{2j} + 1.39\zeta_j, \quad (0 \le j \le 3). \end{aligned} \tag{29, 30}$$

We suppose that the linear approximation expression of delay d, taking into account process variations, is

$$d = d_{00} + \sum_{j=1}^{3} d_{0j} z_j. \tag{31}$$

Using the Galerkin method, we can obtain

$$d_{00} = \frac{\sum\limits_{j=1}^{3} d_{1j}\omega_{nj} - d_{10}\omega_{n0}}{\sum\limits_{j=1}^{3} \omega_{nj}^2 - \omega_{n0}^2},$$

$$d_{0j} = \frac{d_{1j}}{\omega_{n0}} - \frac{\omega_{nj}}{\omega_{n0}} d_0, \quad (0 \le j \le 3). \tag{32}$$

Substituting $z = \{z_1, z_2, z_3\} = \{\Delta W, \Delta T, \Delta H\}$ in Eq. (31), and taking into account process variations, we obtain the RCL statistical delay model

$$d = d_{00} + d_{01}\Delta W + d_{02}\Delta T + d_{03}\Delta H. \tag{33}$$

By observing Eq. (33), we can see that this model is simple in form and can be used in analysis of the impact of process variations on delay. Because ΔW, ΔT, and ΔH are the standard normal distribution and d is the linear function of ΔW, ΔT, and ΔH, d is a normal distribution and its mean and standard deviations are as follows:

$$\mu(d) = d_{00}, \tag{34}$$

$$\sigma(d) = \sqrt{\sum_{j=1}^{3} d_{0j}^2}. \tag{35}$$

This paper transfers nonlinear resistors, capacitors, and inductors to linear form through successive application of the linear approximation method, and then we obtain the linear analytical delay model, which is simple in form. In order to verify the correctness of this model, we apply the distributed RCLG model to simulate the actual non-linear interconnect performance, and compare this model with HSPICE simulation results. As shown in Fig. 3, we take the node 4 as the analysis object. In order to fully consider the inductance effects, we use a step input. Table 1 lists the global interconnect parameters in the different process points.

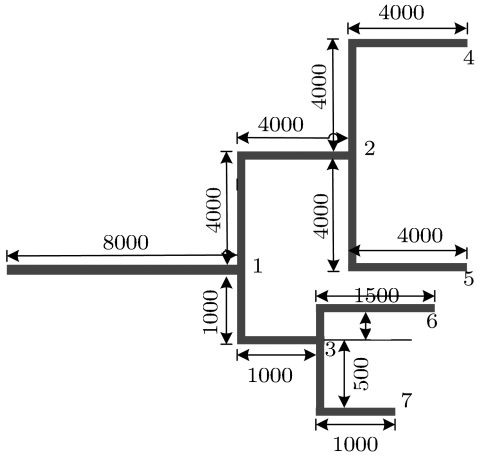


Fig. 3. Global interconnect tree structure (in units of μm).

To illustrate the significant impact of mutual capacitance and mutual inductance on the delay, Table 2 lists the HSPICE simulation delay results of three different cases in the three processes. From Table 2, we can see that mutual capacitance and mutual inductance have an important influence on interconnect delay. If we ignore the role of mutual capacitance and mutual inductance, we will produce large errors which cannot be ignored. At the same time, to validate the model, we use the parameters listed in Table 1. According to international practice, we use a Gaussian distribution to model the process variations. We consider 3σ variations in 30% of the nominal values for each process variable and assume that the variables are independent of each other. We carry out 10000 times Monte–Carlo analysis and measure the 50% delay time.

Table 1. Global interconnect process parameters.[16]

tech. node/nm	45	32	22
width/nm	67.5	48	33
line thickness/nm	162	120	85.8
dielectric thickness/nm	148.5	110.4	79.2
effective conductor resistivity/$\mu\Omega$·cm	3.10	3.52	4.20
effective dielectric constant	2.6–2.9	2.4–2.8	2.1–2.5

Table 2. HSPICE simulation results under three different conditions.

tech. node/nm	delay/ns	delay without mutual capacitance/ns	error/%	delay without mutual inductance/ns	error/%
22	3736.3	712.3	–80.9	3344.0	–10.5
32	1692.3	347.5	–79.5	1501.1	–11.3
45	808.3	177.6	–78.0	721.8	–10.7

Figures 4–6 show respectively the measured delay distribution from the HSPICE simulation and the probability density function of this model during the three different processes. From Figs. 4–6, we can see that this model can accurately simulate the delay distribution taking into account process variations. Table 3 lists the mean and standard deviations of this model and the HSPICE simulation results in three different nano-scale processes. From Table 3 we can see that this model has high precision and the average error when comparing to HSPICE simulation results is less than 3.5%. Therefore, in circuit analysis and design, users can apply this model to estimate the impact of process variations on delay.

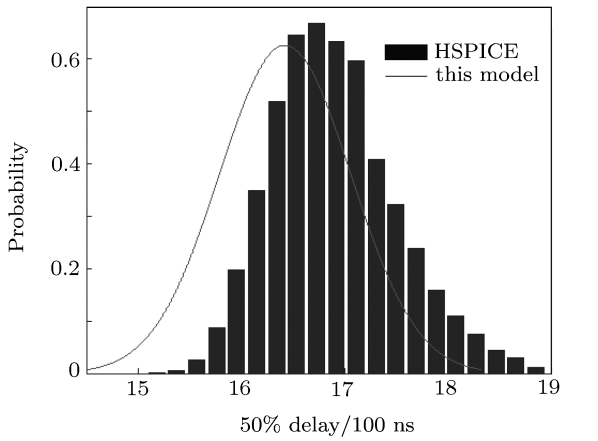


Fig. 5. Comparison between this model and HSPICE in 32 nm process.

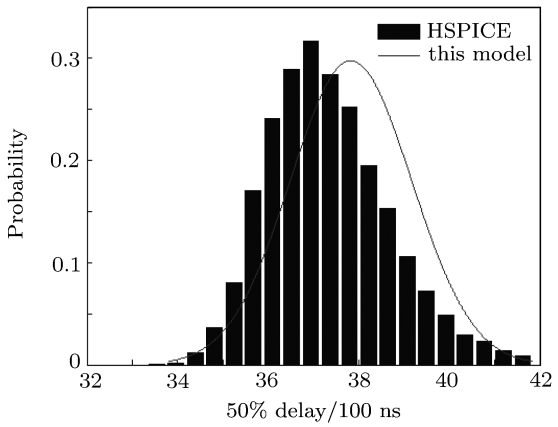


Fig. 4. Comparison between this model and HSPICE in 22 nm process.

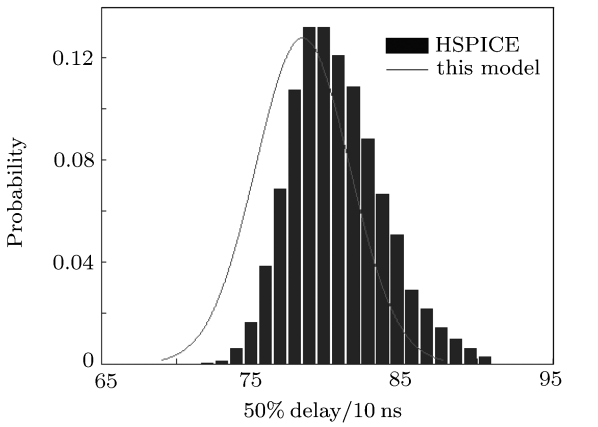


Fig. 6. Comparison between this model and HSPICE in 45 nm process.

Table 3. Comparison between this model and HSPICE in the three kinds of process.

tech. node/nm	μ/ns			σ/ns		
	this model	HSPICE	error/%	this model	HSPICE	error/%
22	3782.8	3736.3	1.24	134.1	138.7	–3.35
32	1642.6	1692.3	–2.94	63.7	65.3	–2.38
45	784.0	808.3	–3.01	31.2	32.3	–3.44

It is worth pointing out that this model is based on the equivalent Elmore delay model, but is independent of the specific form of delay model. When the device size is small, the interconnection parameters show distribution effects and the equivalent Elmore delay model cannot accurately estimate interconnect delay, but the user can successively apply the linear approximation method of this model on the distributed RCL delay model to obtain a more accurate statistical model taking into account process variations.

5. Conclusion

Based on the significant impact of process variations on interconnect performance, this paper presents a linear statistical RCL interconnect delay model which takes into consideration process variations. We first introduce polynomial chaos theory and the Galerkin method. Then, based on the equivalent Elmore delay model and the use of polynomial chaos theory as well as the Galerkin method, we propose a linear statistical RCL interconnect delay model taking into account process variations and successively applying the linear approximation method. HSPICE simulation results validate that the model has higher accuracy. The model is simple and has high precision, and can be used in integrated circuit interconnect system design.

References

[1] Li B, Peh L S and Patra P 2008 *IEEE International Symposium on Networks-on-Chip* (UK: Newcastle University) p125

[2] Lin Y and He L 2008 *IEEE Transaction on Very Large Scale Integration System* **16** 141

[3] Sun P and Luo R 2009 *Proceedings of the 11th International Workshop on System Level Interconnect Prediction* (USA: San Francisco) p19

[4] Raghuandan C, Sainarayanan K S and Srinivas M B 2008 *Proceedings of the 9th International Symposium on Quality Electronic Design* (ISQED) (USA: San Jose) p43

[5] Kim S Y and Wong S S 2007 *IEEE Trans. On Circuits and System* I: *Reg. Papers* **54** 2001

[6] Zhou G, Su L and Jin D 2008 *IEEE 13th Asia and South Pacific Design Automation Conference* (Korea: Soul) p510

[7] Zarrabi H, Al-Khalili A J and Savaria Y 2009 *Proceedings of the 19th ACM Great Lakes Symposium on VLSI* (USA: New York) p45

[8] Elmore W C 1948 *J. Appl. Phys.* **19** 55

[9] Ismail Y I, Friedman E G and Neves J L 2000 *IEEE Transactions on Computer-Aided Design of Integrated Circuits and Systems* **19** 83

[10] Dai W and Hao J 2001 *IEEE International Workshop on Statistical Methodology* (Japan: Kyoto) p51

[11] Ghanem R G and Spanos P 2003 *Stochastic Finite Elements: A Spectral Approach* (New York: Spinger)

[12] Wang J, Ghanta P and Vrudhula S 2004 *Intl. Conf. on Computer-Aided Design* (USA: San Jose) p880

[13] Agarwal K, Agarwal M and Sylvester D 2006 *IEEE Trans. on Computer Aided Design of Integrated Circuits and Systems* **25** 1273

[14] Wong S C, Lee G Y and Ma D J 2000 *IEEE Transactions on Semiconductor Manufacturing* **13** 108

[15] Qi X N, Wang G F and Yu Z P 2000 *IEEE Custom Integrated Circuits Conference* (Florida, USA: Orlando) p487

[16] Semiconductor Industry Association 2007 *International Technology Roadmap for Semiconductors*